PHYSICAL REVIEW D **92,** 055030 (2015)

$SU(2) \times SU(2) \times U(1)$ interpretations of the diboson and Wh excesses

Yu Gao,[1] Tathagata Ghosh,[1] Kuver Sinha,[2] and Jiang-Hao Yu[3]

[1]*Mitchell Institute for Fundamental Physics and Astronomy, Department of Physics and Astronomy, Texas A&M University, College Station, Texas 77843-4242, USA*

[2]*Department of Physics, Syracuse University, Syracuse, New York 13244, USA*

[3]*Theory Group, Department of Physics and Texas Cosmology Center, The University of Texas at Austin, Austin, Texas 78712, USA*

(Received 9 July 2015; published 22 September 2015)

Based on an $SU(2) \times SU(2) \times U(1)$ effective theory framework (aka $G221$ models), we investigate a leptophobic $SU(2)_L \times SU(2)_R \times U(1)_{B-L}$ model in which the right-handed W' boson has the mass of around 2 TeV and predominantly couples to the standard model quarks and the gauge-Higgs sector. This model could explain the resonant excesses near 2 TeV reported by the ATLAS Collaboration in the WZ production decaying into hadronic final states and by the CMS Collaboration in the Wh channel decaying into the $b\bar{b}\ell\nu$ and dijet final state. After imposing the constraints from the electroweak precision and current LHC data, we find that to explain the three excesses in the WZ, Wh, and dijet channels, the $SU(2)_R$ coupling strength g_R favors the range of 0.47–0.68. In this model, given a 2 TeV W' mass, the Z' mass is predicted to favor 2–3 TeV if the doublet Higgs (LPD) is used to break the $G221$ symmetry at the TeV scale and 3–5 TeV for the triplet Higgs (LPT) scenario. Although the LPD Z' might be in tension with the current dilepton resonance searches, the heavier LPT Z' is consistent with current bounds, whose signatures can be further explored by the LHC Run 2 data.

DOI: 10.1103/PhysRevD.92.055030 PACS numbers: 12.60.Cn, 12.60.-i, 14.70.Pw

I. INTRODUCTION

The ATLAS Collaboration has recently reported excesses in searches for massive resonances decaying into a pair of weak gauge bosons [1]. The anomalies have been observed in all hadronic final states in the WZ, WW, and ZZ channels at around 2 TeV invariant mass of the boson pair. The analysis has been done with 20.3 fb^{-1} of data at 8 TeV, with local significances of 3.4σ, 2.6σ, and 2.9σ in the WZ, WW, and ZZ channels, respectively. Several groups [2] have studied this excess. Similar moderate diboson excesses have also been reported from the CMS [3,4] experiment. Intriguingly, the CMS experiment reported around 2σ excesses slightly below 2 TeV in the dijet resonance channel [5] and the $e\nu b\bar{b}$ [6] channel which may arise from a $W' \to Wh$ process.

A natural question to ask is whether a single resonance whose peak is around 2 TeV and width less than 100 GeV can nicely fit all the excesses. The tagging selections used in the analysis do not give a completely clear answer—around 20% of the events are shared among the three channels [1], leading to the possibility of cross-contamination. While a single resonance is definitely the simplest option, a more realistic possibility is that several resonances are present at the 2 TeV mass scale, where new physics presumably kicks in. The most natural scenario is then that these resonances are associated with the spontaneous breaking of extra gauge groups at that scale. Scalars in the extra sectors, for example, would need significant mixing with the standard model Higgs to be reproduced at the LHC and give the observed excesses. The other option is that the resonances are gauge bosons of the new gauge groups, which acquire mass through a Higgs mechanism in the extra sector. This is the avenue we pursue in this paper.

There are several immediate caveats when one considers this possibility. First, extra gauge bosons will decay to the diboson channels through their mixing with the SM W and Z. Such mixing is constrained by electroweak (EW) precision tests necessitating the balance between obtaining the correct cross section to fit the excesses and accommodating EW constraints. The second caveat is that the SM fermions can be charged under the extra gauge group and let the exotic gauge bosons decay into SM fermionic states. One then has to be careful about dilepton and dijet constraints for such a resonance, with the possibility that the former is evaded by working in the context of a leptophobic model. Third, the excess in the ZZ channel cannot be accounted for only with exotic gauge bosons. This makes such scenarios falsifiable in the near future; the persistence of the excess in the ZZ channel would indicate extra physics at the 2 TeV scale, apart from the exotic gauge bosons considered here.

The purpose of this paper is to investigate exotic gauge bosons W' as a candidate for the 2 TeV resonance in light of the caveats mentioned above. In extended gauge group models, usually both the W' boson and the Z' boson exist. We would like to focus on the low-energy effective theory of extended gauge group models in which all the heavy particles other than the W' and Z' bosons decouple. This

has been studied in the $SU(2) \times SU(2) \times U(1)$ framework, as the so-called $G221$ models [7,8]. The $G221$ models are the minimal extension of the SM gauge group to incorporate both the W' and Z' bosons. Various models have been considered under this broad umbrella: left right [9–11], leptophobic (LP), hadrophobic, fermiophobic [7,8,12–14], ununified [15,16], and nonuniversal [17–21].

As an explicit model, we will focus on the LP $G221$ model with two-stage symmetry breaking. In the first-stage breaking, a doublet Higgs (LPD) or a triplet Higgs (LPT) could be introduced. In this model, the W' boson couplings to the SM leptons are highly suppressed. Therefore, this leptophoic model could escape the tight constraints from lepton plus missing energy searches. At the same time, the W' boson couplings to the SM quarks and gauge bosons are similar to the typical left-right model. Therefore, the W' can be produced at the LHC with a potentially large production rate and mainly decays to the dijet, $t\bar{b}$, WZ, and Wh final states instead of the $\ell\nu$ final state. We will explain the resonant excesses near 2 TeV reported by the ATLAS Collaboration in the WZ production decaying into hadronic final states and those reported by the CMS Collaboration in the dijet final state and the Wh channel decaying into the $b\bar{b}\ell\nu$ and dijet final state. Given the W' mass at 2 TeV and the expected signal rate on the WZ final state, the model parameters are fixed. Therefore, we predict the Z' mass and couplings to the SM particles. For the LPD model, the Z' mass is predicted to favor 2–3 TeV and 3–5 TeV for the LPT model. Unlike to the W' boson which is totally leptophobic, the Z' will couple to the SM leptons due to the extra $U(1)$ charge. Therefore, the high-mass dileptonic final state could put constraints on the Z' boson with mass $m_{Z'} < 2.7$–2.8 TeV. We also include the electroweak precision constraints in parameter space. Although some parameter region of the LPD model might be highly constrained due to the dilepton final states, the LPT model could satisfy all the constraints and explain the WZ, Wh, and dijet excesses.

The rest of the paper is structured as follows. In Sec. II, we describe the model in detail. In Sec. III, we describe the constraints on our model coming from electroweak precision tests. In Sec. IV, we describe our main results and predictions. We end with our conclusions.

II. THE $SU(2) \times SU(2) \times U(1)$ MODEL

As mentioned in the Introduction, we will be explicitly working in the context of the $G221$ models [7,8], which we now briefly review. The $G221$ models are the minimal extension of the SM gauge group to incorporate both the W' and Z' bosons. This model can be treated as the low-energy effective theory of extended gauge group models with all the heavy particles other than the W' and Z' bosons decoupled. The gauge structure is $SU(2) \times SU(2) \times U(1)$. There are two kinds of breaking patterns: $SU(2) \otimes U(1)$ breaking down to $U(1)_Y$ (breaking pattern I, where the W' mass is smaller than the Z' mass), and $SU(2) \otimes SU(2)$ breaking down to $SU(2)_L$ (breaking pattern II, where the W' and Z' bosons have the same mass). In breaking pattern I, the model structure is the left-right symmetry $SU(2)_L \times SU(2)_R \times U(1)_X$ with different charge assignments in the fermion sector, while in breaking pattern II, the model includes two left-handed $SU(2)$ with $SU(2)_{L1} \times SU(2)_{L2} \times U(1)_Y$ gauge structure and different charge assignments in the fermion sector. We will mainly be interested in the LP model. In this model, the following symmetry breaking pattern (breaking pattern I) is applied with the gauge structure $SU(2)_L \times SU(2)_R \times U(1)_X$. In the first stage, the breaking $SU(2)_R \times U(1)_X \to U(1)_Y$ occurs at the $\sim$2 TeV scale, while the second stage of symmetry breaking $SU(2)_L \times U(1)_Y \to U(1)_{em}$ takes place at the EW scale.

The gauge couplings for $SU(2)_L$, $SU(2)_R$, and $U(1)_X$ are denoted by g_L, g_R, and g_X, respectively. In the above notation, the gauge couplings are given by

$$g_L = \frac{e}{\sin\theta}, \qquad g_R = \frac{e}{\cos\theta \sin\phi}, \qquad g_X = \frac{e}{\cos\theta \cos\phi}, \tag{1}$$

where the coupling are correlated by the SM weak mixing angle θ and a new mixing angle ϕ. In this model, the SM left-handed fermion doublets are charged under the $SU(2)_L$, and the right-handed quark doublets are charged under the $SU(2)_R$. We identify the $U(1)_X$ as the $U(1)_{B-L}$ gauge symmetry in the following. The charge assignments of the SM fermions are shown in Table I.

At the TeV scale, the $SU(2)_R \times U(1)_{B-L} \to U(1)_Y$ breaking can be induced by a scalar doublet $\Phi \sim (1,2)_{1/2}$ (LPD) or a scalar triplet $(1,3)_1$ (LPT)[1] with a vacuum expectation value (VEV) u. Another bidoublet scalar is introduced for the subsequent $SU(2)_L \times U(1)_Y \to U(1)_Q$ at the EW scale. This is denoted by $H \sim (2,\bar{2})_0$ with two VEVs v_1 and v_2. We will prefer to change variables and work with a single VEV $v = \sqrt{v_1^2 + v_2^2}$ and a mixing angle $\beta = \arctan(v_1/v_2)$. We define a quantity x, which is the ratio of the VEVs

$$x = \frac{u^2}{v^2}, \tag{2}$$

with $x \gg 1$. Usually, the physical observables are not sensitive to the parameter β, as it contributes to physical observables only at the order of $1/x$. So in the following discussion, we will fix $\sin 2\beta$ to be the one to maximize the W' couplings to the gauge bosons and the Higgs boson.

[1]The quantum number assignment is under $[SU(2)_L, SU(2)_R]_{U(1)_{B-L}}$.

TABLE I. The charge assignments of the SM fermions under the leptophobic $G221$ model.

Model	$SU(2)_L$	$SU(2)_R$	$U(1)_{B-L}$
Leptophobic	$\begin{pmatrix} u_L \\ d_L \end{pmatrix}, \begin{pmatrix} \nu_L \\ e_L \end{pmatrix}$	$\begin{pmatrix} u_R \\ d_R \end{pmatrix}$	$\frac{1}{6}$ for quarks $Y_{\rm SM}$ for leptons

The gauge bosons of the $G221$ model are denoted by

$$\begin{aligned} SU(2)_L&: W^{\pm}_{1,\mu}, W^3_{1,\mu}, \\ SU(2)_R&: W^{\pm}_{2,\mu}, W^3_{2,\mu}, \\ U(1)_{B-L}&: X_\mu. \end{aligned} \tag{3}$$

After symmetry breaking, both W' and Z' bosons obtain masses and mix with the SM gauge bosons. To order $1/x$, the eigenstates of the charged gauge bosons are

$$W^{\pm}_{\mu} = W^{\pm}_{1\,\mu} + \frac{\sin\phi \sin 2\beta}{x \tan\theta} W^{\pm}_{2\,\mu}, \tag{4}$$

$$W'^{\pm}_{\mu} = -\frac{\sin\phi \sin 2\beta}{x \tan\theta} W^{\pm}_{1\,\mu} + W^{\pm}_{2\,\mu}. \tag{5}$$

While for the neutral gauge bosons,

$$Z_\mu = W^3_{Z\mu} + \frac{\sin\phi \cos^3\phi}{x \sin\theta} W^3_{H\mu}, \tag{6}$$

$$Z'_\mu = -\frac{\sin\phi \cos^3\phi}{x \sin\theta} W^3_{Z\mu} + W^3_{H\mu}, \tag{7}$$

where W^3_H and W^3_Z are defined as

$$W^3_{H\mu} = \cos\phi W^3_{2\mu} - \sin\phi X_\mu, \tag{8}$$

$$W^3_{Z\mu} = \cos\theta W^3_{1\mu} - \sin\theta(\sin\phi W^3_{2\mu} + \cos\phi X_\mu), \tag{9}$$

$$A_\mu = \sin\theta W^3_{1\mu} + \cos\theta(\sin\phi W^3_{2\mu} + \cos\phi X_\mu). \tag{10}$$

Correspondingly, the masses of the W' and Z' are given by

$$\begin{aligned} M^2_{W'^{\pm}} &= \frac{e^2 v^2}{4\cos^2\theta \sin^2\phi}(x+1), \\ M^2_{Z'} &= \frac{e^2 v^2}{4\cos^2\theta \sin^2\phi \cos^2\phi}(x + \cos^4\phi) \end{aligned} \tag{11}$$

for the LPD model and

$$\begin{aligned} M^2_{W'^{\pm}} &= \frac{e^2 v^2}{4\cos^2\theta \sin^2\phi}(2x+1), \\ M^2_{Z'} &= \frac{e^2 v^2}{4\cos^2\theta \sin^2\phi \cos^2\phi}(4x + \cos^4\phi) \end{aligned} \tag{12}$$

for the LPT model.

For the LPD, the relevant Feynman rules on the fermion couplings are written as

$$W'^{\pm}\bar{f}f': \ \frac{e}{\sqrt{2}\sin\theta}(f_{W'L}P_L + f_{W'R}P_R), \tag{13}$$

with

$$f_{W'L} = -\frac{\sin\phi \sin(2\beta)}{x \tan\theta}, \qquad f_{W'R} = \frac{\tan\theta}{\sin\phi}, \tag{14}$$

and

$$Z'\bar{f}f: \ \frac{e}{\sin\theta\cos\theta}(f_{Z'L}P_L + f_{Z'R}P_R), \tag{15}$$

with

$$f_{Z'L} = (T^3 - Q)\sin\theta\tan\phi - (T^3 - Q\sin^2\theta)\frac{\sin\phi\cos^3\phi}{x\sin\theta}, \tag{16}$$

$$f_{Z'R} = (T^3 - Q\sin^2\phi)\frac{\sin\theta}{\sin\phi\cos\phi} + Q\frac{\sin\theta\sin\phi\cos^3\phi}{x}. \tag{17}$$

For the LPD, the gauge boson self-couplings are given as follows, with all momenta outgoing. The three-point couplings take the form

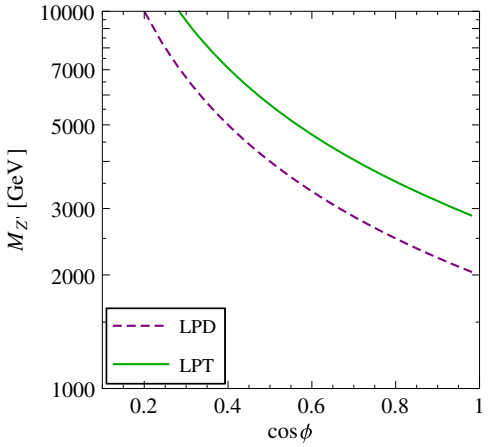

FIG. 1 (color online). Given the W' mass at 2 TeV, the Z' masses in the LPD model and the LPT as a function of the mixing angle $\cos\phi$.

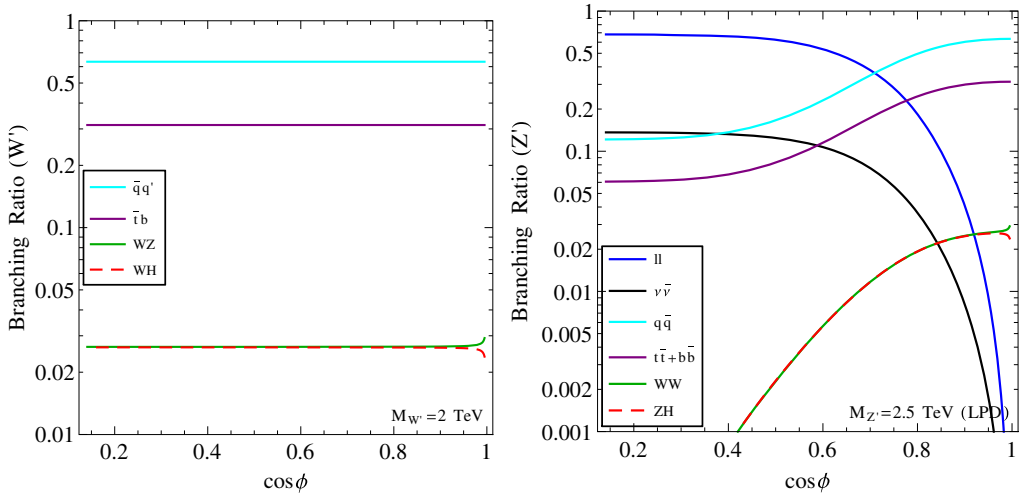

FIG. 2 (color online). The branchings of W' (left panel) and Z' (right panel) to various SM states in the LPD $G221$ model, as a function of the mixing angle $\cos\phi$.

$$V_1^\mu(k_1)V_2^\nu(k_2)V_3^\rho(k_3):$$
$$-if_{V_1V_2V_3}[g^{\mu\nu}(k_1-k_2)^\rho+g^{\nu\rho}(k_2-k_3)^\mu$$
$$+g^{\rho\mu}(k_3-k_1)^\nu], \tag{18}$$

where the coupling strengths $f_{V_1V_2V_3}$ for the WWZ' and $W'WZ$ are

$$f_{WWZ'}=\frac{e\sin\phi\cos^3\phi\cot\theta}{x\sin\theta}, \qquad f_{W'WZ}=\frac{e\sin\phi\sin(2\beta)}{x\sin^2\theta}. \tag{19}$$

Similarly, the HWW' and HZZ' couplings in the LPD are

$$HWW':\ g^{\mu\nu}\frac{e^2v}{2\sin^2\theta}f_{HWW'},$$
$$HZZ':\ g^{\mu\nu}\frac{e^2v}{2\sin^2\theta\cos^2\theta}f_{HZZ'}, \tag{20}$$

with the coupling strengths

$$f_{HWW'}=-\frac{\sin(2\beta)\tan\theta}{\sin\phi}+\frac{\sin(2\beta)(\tan\theta-\cot\theta\sin^2\phi)}{x\sin\phi}, \tag{21}$$

$$f_{HZZ'}=-\frac{\sin\theta}{\tan\phi}+\frac{\cos^3\phi(\sin^2\theta\cos^2\phi-\sin^2\phi)}{x\sin\theta\sin\phi}. \tag{22}$$

For the LPT Feynman rules, the only change to the couplings of the fermion, gauge, and Higgs bosons is to replace x for $2x$ for the W' couplings and replace x for $4x$ for the Z' couplings.

According to Eqs. (11) and (12), the W' mass and the Z' mass are strongly correlated through the mixing angle $\cos\phi$. Given the W' mass and the mixing angle $\cos\phi$, the Z' mass is fully determined. Figure 1 shows the Z' masses in LPD and LPT models as a function of the mixing angle $\cos\phi$, when the W' mass is set to be 2 TeV. As a benchmark point, we will pick up the mixing angle $\cos\phi=0.8$ with $M_{W'}=2$ TeV. Using the above Feynman rules, one can calculate the decay width and branching ratios of W' and Z' to various SM states. The details are shown in the Appendix. For future reference, we display below the branchings for W' and Z' at the point $M_{W'}=2$ TeV and $M_{Z'}=2.5$ TeV, which corresponds to the benchmark point with $\cos\phi=0.8$ in the LPD $G221$ model. From Fig. 2, we also see that the branching ratio $\mathrm{Br}(W'\to WZ)$ is almost equal to the branching ratio $\mathrm{Br}(W'\to Wh)$. This is because when the W' is heavy, the decay products W and Z are highly boosted with the longitudinal polarization $\epsilon_L^\mu(k)\sim k^\mu$. According to the equivalence theorem, we know $\sigma(W'\to WZ)\sim\sigma(W'\to Wh)$. Similarly, we see that $\sigma(Z'\to WW)\sim\sigma(Z'\to Zh)$.

III. ELECTROWEAK PRECISION CONSTRAINTS

In this section, we describe the constraints coming from EW precision tests (EWPTs) [22,23].

In [7,8], a global-fit analysis of 37 EWPTs was performed to derive the allowed model parameter space in the LP $G(221G221)$ model.[2] From Eq. (11), it is clear that $M_{W'}$ and $M_{Z'}$ are not independent parameters. Therefore, $M_{W'}$ was chosen as the input mass. The other independent parameters are the gauge mixing angle ϕ and the mixing angle β. Since the parameter scan is not very sensitive to the

[2]Since there is tree-level mixing between the extra gauge bosons and the SM gauge bosons, all the EWPT data cannot be described by the conventional oblique parameters (S,T,U). A global fit is, thus, performed.

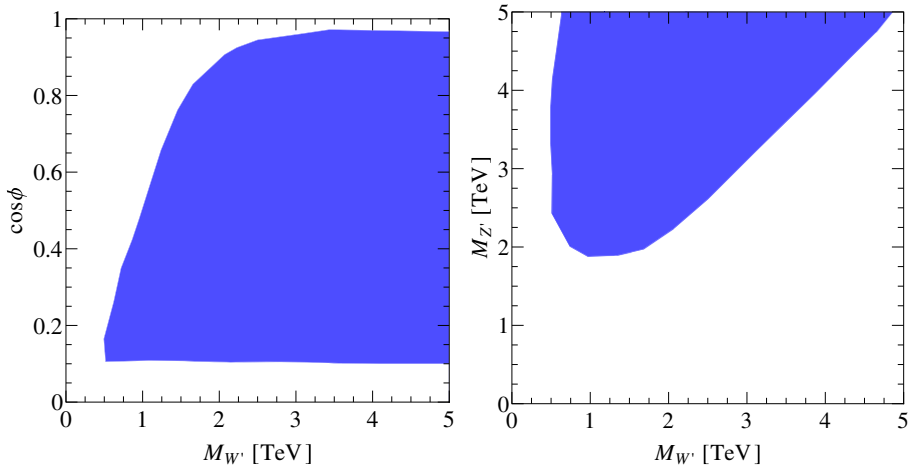

FIG. 3 (color online). Allowed parameter space (blue colored region) of the LPD $G221$ model at 95% C.L. in the $\cos\phi - M_{W'}$ and $M_{Z'} - M_{W'}$ planes after including EWPT constraints.

angle β, which becomes important only at $\mathcal{O}(1/x)$, it can be ignored. Thus, the scans will be presented in the $(M_{W'}, c_\phi)$ plane or the $(M_{W'}, M_{Z'})$ plane.

In Figs. 3 and 4, we show the allowed parameter space (colored region) of the LPD $G221$ model and the LPT $G221$ model, respectively, at 95% C.L. in the $\cos\phi - M_{W'}$ and $M_{Z'} - M_{W'}$ planes after including EWPT constraints.

For both the LPD and LPT models, the allowed region in the $\cos\phi - M_{W'}$ plane shows that direct search constraints favor small $\cos\phi$, which is expected because the W' coupling is proportional to $1/\sin\phi$, leading to a small W' production rate in these regions. However, $\cos\phi$ cannot be too small due to the perturbativity of the g_2 and g_X coupling strength. Conversely, in the $\cos\phi - M_{Z'}$ plane, small $\cos\phi$ is disfavored by direct LHC search constraints because $M_{Z'} \simeq M_{W'}/\cos\phi$.

In the $M_{Z'} - M_{W'}$ plane of Figs. 3 and 4, we can see that in the LPD model with $M_{W'} \sim 2$ TeV, the EWPT constraints force $M_{Z'} \geq 1.9$ TeV, while for the LPT model with $M_{W'} \sim 2$ TeV, the EWPT constraints force $M_{Z'} \geq 2.8$ TeV.

IV. RESULTS AND PREDICTIONS

In this section, we present our main results for explaining the WZ, Wh, and dijet excesses with our model. We discuss, in turn, the results for the W' and Z' bosons.

A. Results for W'

Before proceeding to the W' predictions in our model, we note from Fig. 2 that there is appreciable branching of W' into SM fermions. When resonantly produced in Drell-Yan processes, the $W' \to l\nu$ and $Z' \to ll$ decays lead to tight constraints on the mass of the W' [24] and Z' [25] bosons if their couplings to leptons resemble those between the SM W, Z bosons to SM leptons. In our leptophobic scenario, the leptons are not charged under $SU(2)_R$, and the $W' \to l\nu$ decays are forbidden. Thus, the current W' mass constraint

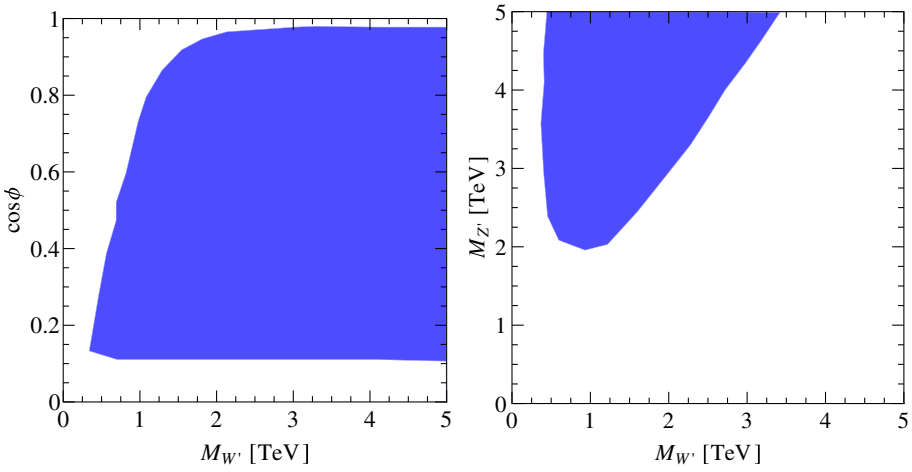

FIG. 4 (color online). Allowed parameter space (blue colored region) of the LPT $G221$ model at 95% C.L. in the $\cos\phi - M_{W'}$ and $M_{Z'} - M_{W'}$ planes after including EWPT constraints.

does not apply to our model. We will see later, however, the $Z' \to ll$ constraint is significant.

First let us focus on the WZ excess. The signal rate in the WZ channel is evaluated as $\sigma_{W'}\mathrm{Br}(W' \to WZ)A_{\mathrm{eff}}$, and A_{eff} is taken to be around 13%, which is the diboson event selection efficiency [1]. Including the event selection efficiency and luminosity, the signal cross section $\sigma_{W'}\mathrm{Br}(W' \to WZ)$ should be around 3–15 fb. Theoretically, the W' production cross section $\sigma_{W'}$ in our $G221$ model can be obtained via the scaling from a next-to-next-to-leading-order (NNLO) "sequential SM" cross section:

$$\sigma_{W'} = \sigma_{\mathrm{NNLO}}\left(\frac{g_{W'L}}{g_{\mathrm{SM}}}\right)^2, \tag{23}$$

where $g_{W'L}$ and g_{SM} denote the W' and SM W coupling to the quarks. We adopt the NNLO W' production cross section from Ref. [24], which is taken to be 292 fb for a sequential SM 2 TeV W'.

Our results for W' are presented in Fig. 5, where we show the cross section times branching ratio for W' in our model as a function of the mixing angle $\cos\phi$ for various channels. From top to bottom, the blue solid, purple solid, green solid, and red dashed lines show the model's prediction signal cross section in the $q\bar{q}'$, $t\bar{b}$, WZ, and Wh channels, respectively. The horizontal shaded yellow band denotes the parameter space compatible with the ATLAS WZ excess with a cross section of 3–15 fb. Thus, a large range of the mixing angle value $0.45 < \cos\phi < 0.92$ can explain the WZ excess.

Given the WZ signal, the equivalence theorem requires the $W' \to Wh$ decay to happen at a comparable rate to that

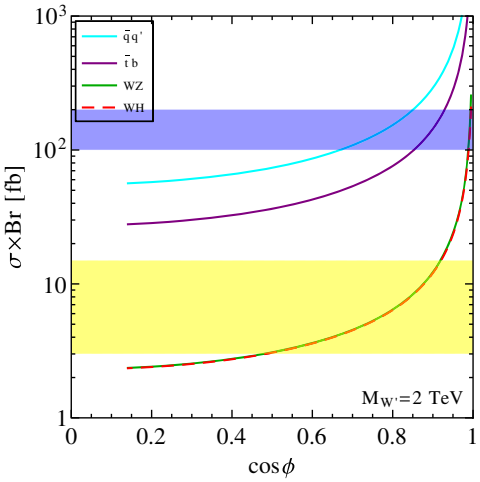

FIG. 5 (color online). The cross section times branching ratio to different channels for a 2 TeV W' as a function of $\cos\phi$. The coincident green and red lines denote the branching times cross section ratio to the WZ and Wh channels. The shaded yellow (blue) band denotes the region that is compatible with the ATLAS WZ (dijet) excess. The WZ and Wh contours overlap due to the Goldstone equivalence theorem.

of the longitudinal polarization of Z in the $W' \to WZ$ process. Since W' is heavy, the daughter Z boson is boosted and dominated by its longitudinal mode. Hence, $\mathrm{BR}(W' \to WZ) \approx \mathrm{BR}(W' \to Wh)$, and an equally large signal in the Wh channel is predicted.

Interestingly, CMS has reported a 2σ up-fluctuation in the $e\nu b\bar{b}$ search [6] that could arise from a 1.8–2.0 TeV W' that decays into Wh. Since the 95% confidence level uncertainty at $M_{W'} = 2$ TeV is given [6] at 8 fb, a 2σ up-fluctuation approximately suggests an 8 fb W' signal. Thus, approximately the same range of $\cos\phi$ that fits the WZ excess would also fit this putative excess. We note that a similar excess in the $\mu\nu b\bar{b}$ channel was not seen [6] in the same analysis. More data will settle the question of whether this excess will be statistically established in the future.

As a benchmark point for these two channels, we choose $\cos\phi = 0.8$. At this point, the cross section times branching ratios of the W' boson to various channels are as follows:

$$\begin{aligned}
\sigma(pp \to W')\mathrm{BR}(W' \to \bar{q}q') &= 150\ \mathrm{fb},\\
\sigma(pp \to W')\mathrm{BR}(W' \to \bar{t}b) &= 71\ \mathrm{fb},\\
\sigma(pp \to W')\mathrm{BR}(W' \to WZ) &= 6.3\ \mathrm{fb},\\
\sigma(pp \to W')\mathrm{BR}(W' \to Wh) &= 6.3\ \mathrm{fb}.
\end{aligned} \tag{24}$$

We now turn to the dijet channel. CMS also reported an $\sim 2\sigma$ up-fluctuation [5] in quark-quark invariant mass at 1.8 TeV. By including the cut efficiency and luminosity, we obtain the dijet excess $\sigma(pp \to W' \to jj)$ around 100–200 fb. If considered as an excess, it is consistent with a sequential SM $W' \to qq$ signal [5]. Our benchmark point yields 30% of the $\sigma\mathrm{BR}(W' \to qq)$ in comparison to the sequential SM case and fits the excess well. In Fig. 5, the horizontal blue band shows the region with a dijet cross section around 100–200 fb that explains the dijet excess. Alternatively, even if the dijet data are interpreted as a bound that marginally excludes a sequential SM W' at 2 TeV, our 2 TeV W' at the benchmark point can still be allowed due to its smaller couplings to the quarks.

It is also interesting to note an associated single top tb final state is also expected at 71 fb, as listed in Eq. (24). While still below current LHC limits [26], it can be searched at future high statistics runs.

In conclusion, we see that after imposing the constraints from EWPT and current LHC data, we can explain the WZ, Wh, and dijet excesses together for a range of values of the $SU(2)_R$ coupling strength g_R in the range 0.47–0.68, which corresponds to the range $0.66 < \cos\phi < 0.85$.

B. Results for Z'

We now turn to constraints on the Z' boson in our model and comment on the possibility of explaining the WW excess. Since we know the favored region of the W' mass and the mixing angle $\cos\phi$, the favored Z' mass and

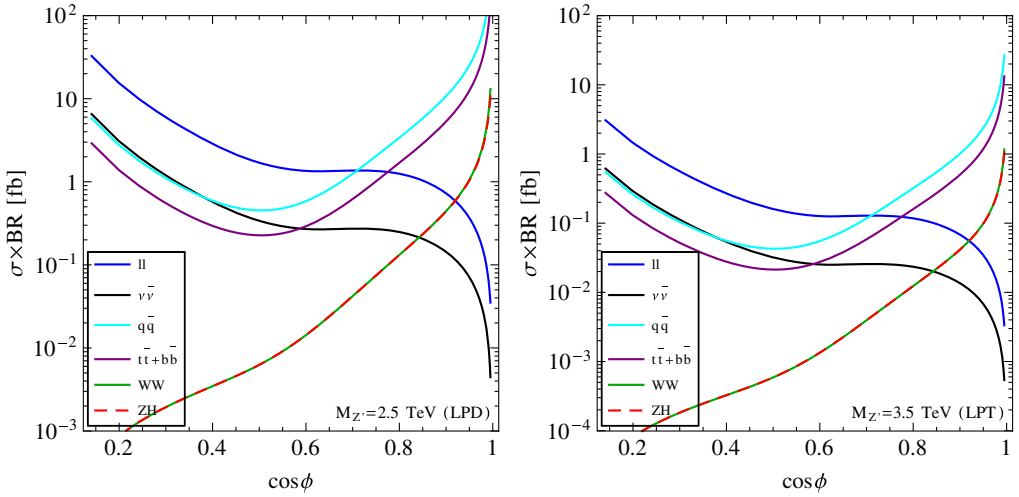

FIG. 6 (color online). The cross section times branching to different channels for Z' in the doublet model (left panel) and the triplet model (right panel), as a function of $\cos\phi$.

couplings could be fully predicted. Using our benchmark point with $\cos\phi = 0.8$, the Z' mass is predicted to be 2.5 TeV for the LPD model and 3.5 TeV for the LPT model. Our main results for the Z' boson in the benchmark point are summarized in Fig. 6. In the left panel, we show the results for the LPD model and the right panel shows the LPT model.

First, we consider the dilepton constraint in the two charged lepton channel relevant for $Z' \to ll$. The leptons in our model are charged under $U(1)$, and, thus, $Z' \to ll$ processes can occur via the Z' mixing with Z. In ATLAS's recent dilepton analysis [25,27], the Z' mass with sequential SM couplings is constrained to 2.7–2.8 TeV at 95% confidence level.

In the LPD case, Fig. 1 shows the Z' mass is around 2–3 TeV in the favored $\cos\phi$ region from the W': $0.66 < \cos\phi < 0.85$. Figure 6 shows that the EWPT constraints allow a Z' mass as low as 2.1 TeV for $M_{W'} \sim 2$ TeV. For this lower Z' mass to be consistent with the dilepton search bound, Z' must either have a small production cross section, i.e., smaller couplings to quarks, and/or a lower decay branching ratio into leptons than a sequential SM Z' does. The combination of these two factors can be optimized by varying the $\cos\phi$ value. At the benchmark point $\cos\phi = 0.8$, which corresponds to $M_{Z'} = 2.5$ TeV, the cross section times branching ratios for the various channels are as follows:

$$\begin{aligned}
\sigma(pp \to Z')\mathrm{BR}(Z' \to \bar{q}q') &= 3.56 \text{ fb}, \\
\sigma(pp \to Z')\mathrm{BR}(Z' \to \bar{t}t(\bar{b}b)) &= 1.78 \text{ fb}, \\
\sigma(pp \to Z')\mathrm{BR}(Z' \to ll) &= 1.22 \text{ fb}, \\
\sigma(pp \to Z')\mathrm{BR}(Z' \to \nu\bar{\nu}) &= 0.25 \text{ fb}, \\
\sigma(pp \to Z')\mathrm{BR}(Z' \to Zh) &= 0.13 \text{ fb}, \\
\sigma(pp \to Z')\mathrm{BR}(Z' \to WW) &= 0.13 \text{ fb}. \qquad (25)
\end{aligned}$$

We found a minimal Z' production at 21% of the sequential SM cross section and the lowest $\mathrm{BR}(Z' \to ll) = 12\%$ within EWPT constraints, which are too large to evade the $Z' \to ll$ constraint. To evade this tight constraint, we need the Z' mass to be greater than 2.8 TeV. This is possible in the LPD model if the model takes a smaller $\cos\phi$: $0.66 < \cos\phi < 0.72$. From Fig. 5, the smaller $\cos\phi$, the smaller the cross section times branching ratio for a 2 TeV W'. Therefore, to explain the WZ, Wh, and dijet excesses and escape the dilepton constraint in the LPD model, one needs the mixing angle to be around $0.66 < \cos\phi < 0.72$.

In the LPT model, Fig. 1 shows the Z' mass is around 3–5 TeV in the favored $\cos\phi$ region. This Z' is beyond the search limits of the current dilepton bound. As shown in Fig. 4, the EWPT constraints in the LPT scenario allow $M_{Z'} \geq 2.8$ TeV for $M_{W'} \sim 2$ TeV. Therefore, the LPT model is totally consistent with the ATLAS dilepton bound. However, such a large Z' mass would be unsuitable to explain the diboson WW excess.

In conclusion, we find that the LPD scenario predicts a Z' boson with mass around 2–3 TeV, which is compatible with EWPT but is tightly constrained by the dilepton searches, except for the parameter region with $0.66 < \cos\phi < 0.72$, which corresponds to $M_{Z'} > 2.8$ TeV. We also note that the LPT scenario predicts a Z' boson with mass around 3–5 TeV that is completely compatible with EWPT and LHC dilepton constraints, which, however, would be irrelevant for the recent WW diboson excess.

V. CONCLUSIONS

We investigated the prospects of the leptophobic $SU(2)_L \times SU(2)_R \times U(1)_{B-L}$ model as a potential explanation of the diboson and Wh excesses. In our discussion, we fixed the W' mass to be 2 TeV. Within the electroweak precision data limits, we found that to explain the WZ, Wh,

and dijet excesses together, the $SU(2)_R$ coupling strength g_R favors the range of 0.47–0.68 and a range for mixing angle $0.66 < \cos\phi < 0.85$. We noticed that the Z' mass and couplings are determined by the two parameters that appeared in the W' sector. Therefore, given the favored region to explain the excesses, the Z' masses were determined to be around 2–3 TeV for the LPD model and 3–5 TeV for LPT model, and the Z' decay widths to the dilepton, dijet, and gauge bosons were predicted. We found the ATLAS WW and ZZ excesses are unlikely to arise from the heavy Z' from this model due to a much heavier Z' mass in the LPT model. We also investigated the constraints from current $Z' \to ll$ searches and electroweak precision data and found that although the LPD Z' might be in tension with the current dilepton resonance searches, the heavier LPT Z' is consistent with current bounds.

As a model-independent check, the leptonic decay of the $W' \to WZ$ bosons would lead to a $3l + E_{\mathrm{T}}$ final state with the same invariant mass around 2 TeV. No significant excess has been reported in this channel, and the current CMS [28] data place a constraint of $\sigma \times \mathrm{BR}(W' \to 3l\nu)$ below 0.1 fb for $M_{W'} = 2$ TeV. Given the SM WZ leptonic decay branching fractions, the relative size of the four-jet final state is 0.03. If the four-jet WZ excess persists, an associated $\sigma_{W'}\mathrm{BR}(W' \to 3l\nu)$ excess at 0.2 fb is expected. Also, no significant deviation from the SM was observed from ATLAS's recent analysis [29,30] of the semileptonic $WZ/WW \to l\nu jj$ channel. It is noted that many of the aforementioned up-fluctuations are statistically limited in the current data, and LHC Run 2 updates will greatly help confirm or clarify the excesses.

In summary, the recent tantalizing excesses in the WZ, Wh, and dijet channels can be accommodated with the LPT model and a limit range of parameter space of the LPD model in a manner consistent with both EWPT and LHC constraints.

ACKNOWLEDGMENTS

We would like to thank the CETUP 2015 Dark Matter Workshop in South Dakota for providing a stimulating atmosphere where this work was conceived and concluded. Y. G. thanks the Mitchell Institute for Fundamental Physics and Astronomy for support. T. G. is supported by Department of Energy Grant No. DE-FG02-13ER42020. K. S. is supported by National Aeronautics and Space Administration Astrophysics Theory Grant No. NNH12ZDA001N. The research of J. H. Y. is supported by the National Science Foundation under Grants No. PHY-1315983 and No. PHY-1316033.

APPENDIX: HEAVY GAUGE BOSON DECAY WIDTH

The partial decay width of $V' \to \bar{f}_1 f_2$ is

$$\Gamma_{V'\to\bar{f}_1 f_2} = \frac{M_{V'}}{24\pi}\beta_0\left[(g_L^2+g_R^2)\beta_1 + 6g_L g_R\frac{m_{f_1}m_{f_2}}{M_{V'}^2}\right]\Theta(M_{V'} - m_{f_1} - m_{f_2}), \tag{A1}$$

where

$$\beta_0 = \sqrt{1 - 2\frac{m_{f_1}^2 + m_{f_2}^2}{M_{V'}^2} + \frac{(m_{f_1}^2 - m_{f_2}^2)^2}{M_{V'}^4}},$$
$$\beta_1 = 1 - \frac{m_{f_1}^2 + m_{f_2}^2}{2M_{V'}^2} - \frac{(m_{f_1}^2 - m_{f_2}^2)^2}{2M_{V'}^4}. \tag{A2}$$

The color factor N_c is not included, and the top quark decay channel is only open when the Z' and W' masses are heavy.

The partial decay width of $V' \to V_1 V_2$ is

$$\Gamma_{V'\to V_1 V_2} = \frac{M_{V'}^5}{192\pi M_{V_1}^2 M_{V_2}^2} g_{V'V_1V_2}^2 \beta_0^3 \beta_1 \Theta(M_{V'} - M_{V_1} - M_{V_2}), \tag{A3}$$

where

$$\beta_0 = \sqrt{1 - 2\frac{M_{V_1}^2 + M_{V_2}^2}{M_{V'}^2} + \frac{(M_{V_1}^2 - M_{V_2}^2)^2}{M_{V'}^4}},$$
$$\beta_1 = 1 + 10\frac{M_{V1}^2 + M_{V2}^2}{2M_{V'}^2} + \frac{M_{V_1}^4 + 10M_{V1}^2M_{V_2}^2 + M_{V_2}^4}{M_{V'}^4}. \tag{A4}$$

The partial decay width of $V' \to V_1 H$ (where $V_1 = W$ or Z boson and H is the lightest Higgs boson) is

$$\Gamma_{V'\to V_1 H} = \frac{M_{V'}}{192\pi}\frac{g_{V'V_1H}^2}{M_{V_1}^2}\beta_0\beta_1\Theta(M_{V'} - M_{V_1} - M_{V_2}), \tag{A5}$$

where

$$\beta_0 = \sqrt{1 - 2\frac{M_{V_1}^2 + m_H^2}{M_{V'}^2} + \frac{(M_{V_1}^2 - m_H^2)^2}{M_{V'}^4}},$$
$$\beta_1 = 1 + \frac{10M_{V_1}^2 - 2m_H^2}{2M_{V'}^2} + \frac{(M_{V_1}^2 - m_H^2)^2}{M_{V'}^4}. \tag{A6}$$

[1] G. Aad *et al.* (ATLAS Collaboration), arXiv:1506.00962.

[2] H. S. Fukano, M. Kurachi, S. Matsuzaki, K. Terashi, and K. Yamawaki, arXiv:1506.03751; J. Hisano, N. Nagata, and Y. Omura, arXiv:1506.03931 [Phys. Rev. D (to be published)]; D. B. Franzosi, M. T. Frandsen, and F. Sannino, arXiv:1506.04392; K. Cheung, W. Y. Keung, P. Y. Tseng, and T. C. Yuan, arXiv:1506.06064; S. S. Xue, arXiv:1506.05994; B. A. Dobrescu and Z. Liu, arXiv:1506.06736; J. A. Aguilar-Saavedra, arXiv:1506.06739.

[3] V. Khachatryan *et al.* (CMS Collaboration), J. High Energy Phys. 08 (2014) 173.

[4] V. Khachatryan *et al.* (CMS Collaboration), J. High Energy Phys. 08 (2014) 174.

[5] V. Khachatryan *et al.* (CMS Collaboration), Phys. Rev. D **91**, 052009 (2015).

[6] CMS Collaboration, Report No. CMS-PAS-EXO-14-010, 2014.

[7] K. Hsieh, K. Schmitz, J. H. Yu, and C.-P. Yuan, Phys. Rev. D **82**, 035011 (2010).

[8] Q. H. Cao, Z. Li, J. H. Yu, and C. P. Yuan, Phys. Rev. D **86**, 095010 (2012).

[9] R. N. Mohapatra and J. C. Pati, Phys. Rev. D **11**, 2558 (1975).

[10] R. N. Mohapatra and J. C. Pati, Phys. Rev. D **11**, 566 (1975).

[11] R. N. Mohapatra and G. Senjanovic, Phys. Rev. D **23**, 165 (1981).

[12] R. S. Chivukula, B. Coleppa, S. Di Chiara, E. H. Simmons, H. J. He, M. Kurachi, and M. Tanabashi, Phys. Rev. D **74**, 075011 (2006).

[13] V. D. Barger, W. Y. Keung, and E. Ma, Phys. Rev. D **22**, 727 (1980).

[14] V. D. Barger, W. Y. Keung, and E. Ma, Phys. Rev. Lett. **44**, 1169 (1980).

[15] H. Georgi, E. E. Jenkins, and E. H. Simmons, Phys. Rev. Lett. **62**, 2789 (1989); **63**, 1540 (1989).

[16] H. Georgi, E. E. Jenkins, and E. H. Simmons, Nucl. Phys. **B331**, 541 (1990).

[17] X. Li and E. Ma, Phys. Rev. Lett. **47**, 1788 (1981).

[18] D. J. Muller and S. Nandi, Phys. Lett. B **383**, 345 (1996).

[19] E. Malkawi, T. M. P. Tait, and C. P. Yuan, Phys. Lett. B **385**, 304 (1996).

[20] X. G. He and G. Valencia, Phys. Rev. D **66**, 013004 (2002).

[21] E. L. Berger, Q. H. Cao, J. H. Yu, and C.-P. Yuan, Phys. Rev. D **84**, 095026 (2011).

[22] A. Abele *et al.* (Crystal Barrel Collaboration), Eur. Phys. J. C **19**, 667 (2001).

[23] J. Erler, arXiv:hep-ph/0005084.

[24] G. Aad *et al.* (ATLAS Collaboration), J. High Energy Phys. 09 (2014) 037.

[25] G. Aad *et al.* (ATLAS Collaboration), Phys. Rev. D **90**, 052005 (2014).

[26] G. Aad *et al.* (ATLAS Collaboration), Phys. Lett. B **743**, 235 (2015); G. Aad *et al.* (ATLAS Collaboration), Eur. Phys. J. C **75**, 165 (2015).

[27] S. Patra, F. S. Queiroz, and W. Rodejohann, arXiv:1506.03456.

[28] V. Khachatryan *et al.* (CMS Collaboration), Phys. Lett. B **740**, 83 (2015).

[29] G. Aad *et al.* (ATLAS Collaboration), Eur. Phys. J. C **75**, 209 (2015).

[30] G. Aad *et al.* (ATLAS Collaboration), Eur. Phys. J. C **75**, 69 (2015).